

Structural Basis of Nanomolar Inhibition of Tumor-Associated Carbonic Anhydrase IX: X-Ray Crystallographic and Inhibition Study of Lipophilic Inhibitors with Acetazolamide Backbone

Jacob T. Andring, Mallorie Fouch, Suleyman Akocak, Andrea Angeli, Claudiu T. Supuran,*
Marc A. Ilies,* and Robert McKenna*

Cite This: <https://dx.doi.org/10.1021/acs.jmedchem.0c01390>

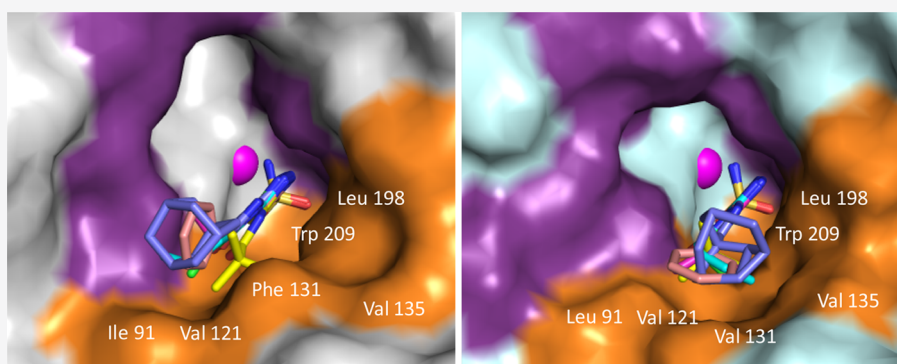
Read Online

ACCESS |

Metrics & More

Article Recommendations

Supporting Information



ABSTRACT: This study provides a structure–activity relationship study of a series of lipophilic carbonic anhydrase (CA) inhibitors with an acetazolamide backbone. The inhibitors were tested against the tumor-expressed CA isozyme IX (CA IX), and the cytosolic CA I, CA II, and membrane-bound CA IV. The study identified several low nanomolar potent inhibitors against CA IX, with lipophilicities spanning two log units. Very potent pan-inhibitors with nanomolar potency against CA IX and sub-nanomolar potency against CA II and CA IV, and with potency against CA I one order of magnitude better than the parent acetazolamide **1** were also identified in this study, together with compounds that displayed selectivity against membrane-bound CA IV. A comprehensive X-ray crystallographic study (12 crystal structures), involving both CA II and a soluble CA IX mimetic (CA IX-mimic), revealed the structural basis of this particular inhibition profile and laid the foundation for further developments toward more potent and selective inhibitors for the tumor-expressed CA IX.

INTRODUCTION

A common feature of many aggressive tumors is hypoxia.¹ Fast tumor growth places many tumor cells sufficiently far from blood vessels resulting in an inadequate amount of oxygen. As a consequence, the hypoxia-inducible factor 1 (HIF-1) is upregulated in hypoxic tumor cells, relocates to the nucleus, and triggers the expression of a group of proteins needed for the adaptation of cancer cells to survive the hypoxic environment.² Among them, carbonic anhydrase isozyme IX (CA IX) plays a key role in maintaining tumor cell pH homeostasis.^{3–10}

Carbonic anhydrases (CAs) are a family of zinc metalloenzyme that catalyzes the reversible hydration of carbon dioxide to bicarbonate ion and a proton ($\text{CO}_2 + \text{H}_2\text{O} \rightleftharpoons \text{HCO}_3^- + \text{H}^+$). These isozymes have different subcellular localizations, such as cytosolic (CA I–III, VII, XIII), mitochondrial (CA VA, VB), membrane-bound (CA IV, IX, XII, XIV, and XV), or secreted (CA VI). Through each of these CA isozymes, cells can quickly equilibrate the intra-

cellular and extracellular $\text{CO}_2/\text{HCO}_3^-$ pools.^{3,5} The distribution of CA isozymes in humans differs from one isozyme to another, with CA isozymes ubiquitously present in most cell and tissue types (e.g., CA I, CA II), in specific organs (e.g., CA IV in lungs, kidneys, ciliary processes of the eye), while others have a relatively restricted tissue distribution (e.g., CA IX only expressed in the epithelium lining the stomach and the small intestine in normal physiology).^{3,11} However, CA IX as well as CA XII have been identified as potential cancer targets. As mentioned previously, the CA IX isozyme is upregulated in tumors,^{5,12–14} where it functions to maintain the extracellular

Received: August 18, 2020

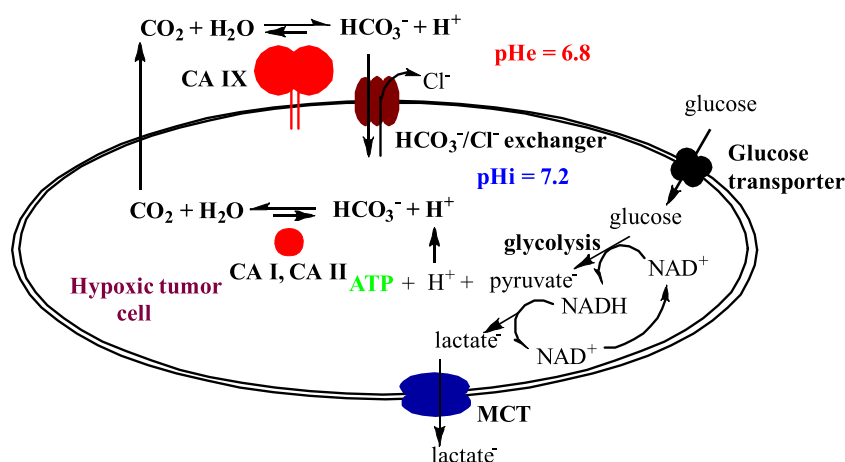
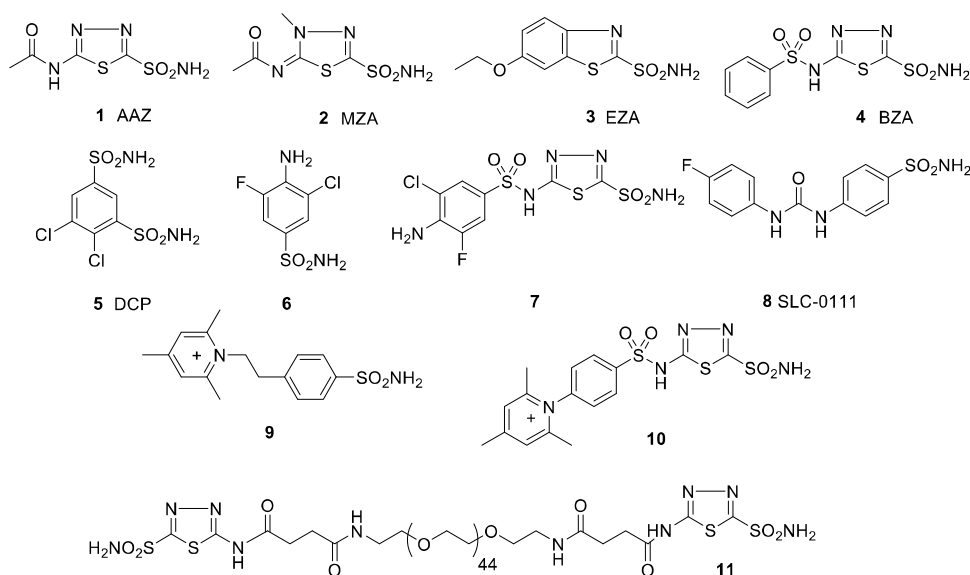


Figure 1. Biochemistry of hypoxic tumor cells: ATP is produced in the absence of oxygen through the upregulation of glycolysis, which also produces pyruvate and protons. Pyruvate is converted to lactate, regenerating NAD^+ needed for glycolysis, and then lactate is excreted through monocarboxylate transporter (MCT). Intracellular pH homeostasis is maintained without ATP consumption *via* the action of CA isozymes: ubiquitously expressed cytosolic CA I, CA II, and the extracellular membrane-bound CA IX, which is overexpressed in hypoxic tumors. Efficient inhibition of CA IX has thus the potential to kill tumor cells.

Chart 1. CA Inhibitors Used in the Clinics, Together with Some Representative CAIs with High Potency against Membrane-Bound CA Isozymes, Including CA IX



pH homeostasis within normal limits, despite significant upregulation of glycolysis with increased H^+ production. Thus, in the cytoplasm of hypoxic tumor cells, CA I and CA II catalyze the conversion of glycolytic protons with cytoplasmic HCO_3^- to yield CO_2 and H_2O . CO_2 passes through the cell membrane and is rehydrated in the extracellular environment of the tumor by the overexpressed CA IX, reforming the HCO_3^- and H^+ ions. The bicarbonate ion is subsequently imported into the cytoplasm *via* the anion exchanger AE2, which exports Cl^- in exchange for HCO_3^- . As a net result of the action of CA IX, in tandem with CA I, CA II, and AE2, hypoxic tumor cells can ensure pH homeostasis despite the upregulated glycolysis, efficiently exporting the glycolytic protons in the extracellular milieu without ATP consumption (Figure 1).¹⁵ This key biochemical mechanism allows malignant cells to secure the energy needed for continuous growth and proliferation under hypoxic conditions.^{16–18} Thus, CA IX expression has been associated

with poor prognosis in colorectal,^{14,19,20} breast,^{12,21,22} ovarian,^{23,24} pancreatic,²⁵ head and neck,²⁶ cervical,^{27,28} brain,²⁹ and bladder cancers.³⁰ Inhibition of CA IX has proved to be a viable strategy to fight these aggressive metastatic tumors.^{3,5,31,32}

However, clinically used CA inhibitors (Chart 1) such as aromatic and heterocyclic primary sulfonamide acetazolamide (1, AAZ), methazolamide (2, MZA), ethoxzolamide (3, EZA), benzolamide (4, BZA), or dichlorphenamide (5, DCP), although relatively potent against CA IX,³ have suboptimal pharmacokinetic and biodistribution profiles due to their hydrophilic nature, being essentially designed to inhibit CA isozymes in kidneys (CA II, CA IV) and to act primarily as diuretics.³³ It was shown by our team that one can conjugate the benzenesulfonamide and 1,3,4-thiadiazole-2-sulfonamide zinc-binding motifs with different hydrophilic, amphiphilic, or hydrophobic moieties^{34–38} to increase the potency and selectivity of the resulting CA inhibitors (CAIs) by exploiting

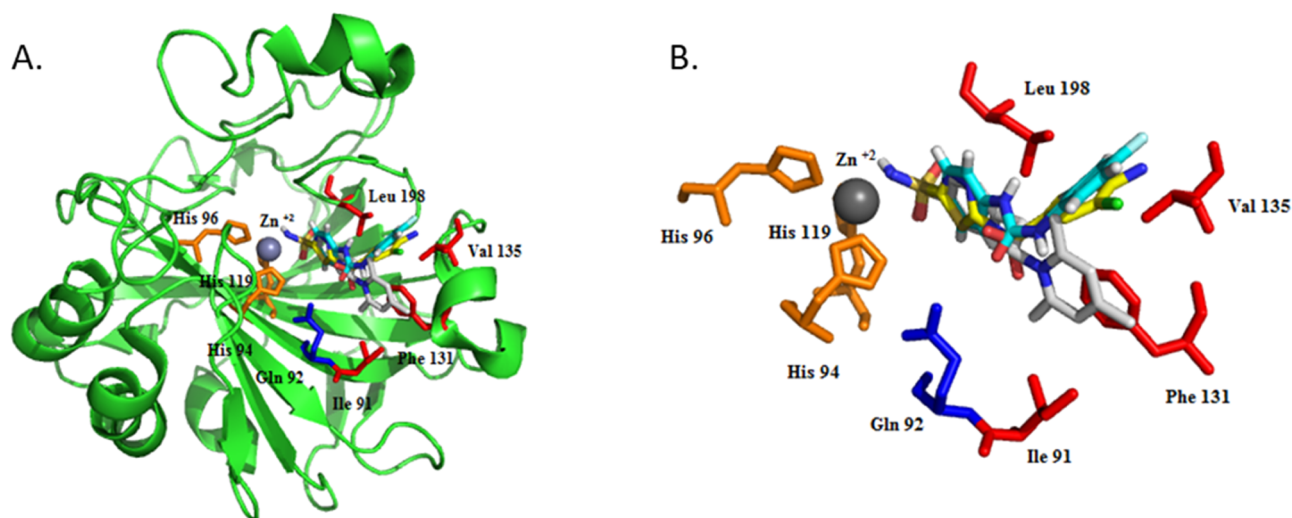
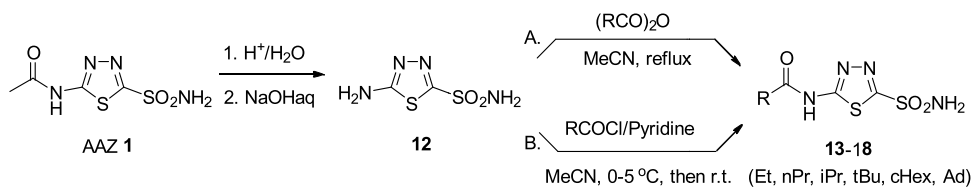


Figure 2. Ribbon diagram (A) and active site details (B) of the 7/CAII (PDB 2HOC,⁵⁸ rendered in light yellow), 8/CA II (PDB 3N4B,⁵⁴ rendered in light blue), 9/CA II (PDB 1ZE8,⁶² rendered in gray) adducts (superimposed), revealing the orientation of the tail of the inhibitor either toward P1 (defined by residues Phe131, Val135, Leu198) for CAIs 7, 8 or P2 (defined by residues Ile91, Gln92, Phe131) for CAI 9.

Scheme 1. Synthetic Strategy for the Generation of Lipophilic CA Inhibitors 13–18, Starting from Acetazolamide



the additional interactions of these moieties with key residues in the active site of CA isozymes in the so-called “tail approach” to potent and selective CAIs.³⁹ We applied this strategy to CA IX isozyme by synthesizing the halogenated aromatic and heterocyclic sulfonamides **6**, **7** and congeners, in the first CA IX inhibition study with synthetic inhibitors (Chart 1).³² The same tail approach also yielded the ureido and thioureido sulfonamides as potent CAIs,³⁶ and subsequent modulation of lipophilicity through halogen decoration yielded powerful CA IX inhibitors such as **8**.⁴⁰ Other strategies involve conjugation of CAIs with charged groups (as in CAIs **9** and **10**)^{34,35,37,41,42} with sugar^{43–47} or with polymeric moieties (as **11**, Chart 1).⁴⁸ These lead compounds demonstrated the ability to inhibit CA IX and control the growth of various carcinomas *in vitro* and *in vivo*.^{45,49–51} Compound **8** (SLC-0111) was proved to be efficient against metastatic breast cancer^{40,52–54} and is currently in advanced clinical trials for the treatment of hypoxic tumors that overexpress CA IX (Chart 1).^{3–5,49,55} The strategy was successfully used for the generation of many potent CA IX inhibitors.^{3,5,46,51,55–57}

In parallel with these synthetic efforts, we also conducted X-ray crystallographic studies with these lead compounds to reveal their binding in the active site of CAs and to elucidate the structural basis of their potency and selectivity.^{5,58–61} Thus, crystal structures of the adducts of 7/CAII (PDB 2HOC⁵⁸), 8/CA II (PDB 3N4B⁵⁴), 9/CA II (PDB 1ZE8⁶²), and related^{5,58–61} reveal that the tail approach is exploiting the binding of the elongated CAIs in two major binding pockets, denominated P1 and P2 (Figure 2).^{5,58,62–64} The first binding pocket, denominated P1, is defined by residues Phe131, Val135, and Leu198, while the second pocket, denominated P2, is defined by residues Phe131, Ile91, and Gln92 (Figure

2).^{5,58,62–64} These crystallographic studies helped toward the design of more potent CA IX inhibitors^{57,65–69} and benefitted from the crystallization of the catalytic domain of CA IX⁷ and by the creation of a CA IX mimic by replacing the key amino acid residues in the active site of CA II with the corresponding ones found in the CA IX structure.⁷⁰ The abovementioned crystallographic studies evidenced that there are major structural differences between ubiquitous CA II and tumor-overexpressed CA IX at the level of P2 site. CA II has a Phe in position 131, which restricts the P2 site in this isozyme, while CA IX has a Val, which makes the P2 site in this isozyme much larger.

One can notice that this site is also hydrophobic, pointing to the fact that one can increase simultaneously the potency and the selectivity of a CAI toward CA IX through the use of lipophilic moieties, which can locate either in the P1 or in the P2 site. Therefore, we have decided to systematically investigate the effect of conjugating the 2-amino-5-sulfonamido-1,3,4-thiadiazole pharmacophore of acetazolamide with lipophilic moieties of increased size toward inhibition of CA IX, in a comparative manner with ubiquitously spread CA II and to double this synthetic and inhibition study with a comprehensive X-ray crystallographic study on CA II and CA IX.

RESULTS AND DISCUSSION

The new CAIs were synthesized starting from the same key intermediate 2-amino-5-sulfonamido-1,3,4-thiadiazole **12** *via* acylation with the corresponding acid chlorides in the presence of pyridine as base, in acetonitrile (method A), or with the corresponding acid anhydrides in acetonitrile, at reflux (method B). The key intermediate **12** was synthesized from

acetazolamide (AAZ) **1** via acid deprotection, followed by neutralization of the corresponding hydrochloride (Scheme 1). CAIs **13–18** were purified by flash chromatography, crystallized, and characterized by standard analytical methods (see the Materials section).

The lipophilic CAIs **13–18** were tested for their ability to inhibit the tumor-overexpressed CA IX isozyme, the ubiquitous cytosolic CA I and CA II isozymes, and the membrane-bound isozyme CA IV that can be reached *in vivo* by compounds **13–18**. The parent Acetazolamide **1** was also included for comparison (Table 1). Data from Table 1

Table 1. Physicochemical Properties and Inhibition Data against Human CA Isoforms CA I, II, IV, and IX with Derivatives 13–18 Reported Here and with the Standard Inhibitor Acetazolamide (AAZ, 1) by a Stopped-Flow CO₂ Hydrase Assay

| comp | R | log <i>P</i> | <i>K_i</i> (nM) ^a | | | |
|--------------|-------------|--------------|--|-------|-------|-------|
| | | | CA I | CA II | CA IV | CA IX |
| AAZ 1 | Me | 0.14 | 250 | 12.1 | 74 | 25.8 |
| 13 | Et | 0.8 | 66.8 | 2.7 | 0.78 | 12.8 |
| 14 | nPr | 1.21 | 53.8 | 0.52 | 0.37 | 2.1 |
| 15 | <i>i</i> Pr | 1.36 | 75.1 | 0.59 | 0.44 | 2.4 |
| 16 | <i>t</i> Bu | 2.07 | 63.4 | 0.66 | 0.43 | 8.2 |
| 17 | cHex | 2.12 | 62.8 | 0.53 | 0.36 | 15.7 |
| 18 | Ad | 2.28 | 883 | 11.0 | 349 | 6.4 |

^aMean from three different assays, by a stopped-flow technique (errors were in the range of ±5–10% of the reported values). Monomeric (recombinant) human enzymes used in all cases.

revealed an excellent inhibitory profile of compounds **13–18** against CA II, CA IV, and CA IX, with nanomolar and even sub-nanomolar potency of some representatives against these targets. The CA I isozyme was the least susceptible to be inhibited with CAIs **13–18**. The inhibitory potency of the new compounds increased while elongating the tail length from Me (AAZ **1**) to Et (**13**) and nPr (**14**). Tail branching to *i*Pr (compound **15**), *t*Bu (compound **16**), or cHexyl (compound **17**) does not significantly increase the potency of the CAI toward CA I. However, the substitution of cHexyl moiety from **17** with much bulkier adamantyl (Ad in Scheme 1) in **18** lowers the inhibitory potency with 1 order of magnitude (Table 1). The same trend is valid for the other three isozymes: the initial elongation of the tail of the inhibitor increases the potency of the inhibitor, with nPr congener **14** being the most potent representative against CA II, IV, and IX, and reaching low nanomolar potency for CA IX and sub-nanomolar potency for CA II and CA IV. Branching of the tail in *i*Pr (compound **15**), *t*Bu (compound **16**), and cHexyl (compound **17**) does not alter much the inhibitory potency against CA II and CA IV, which remain sub-nanomolar. However, CA IX seems to be more sensitive to this branching effect, with *K_i*'s values increasing from nPr congener **14** to *i*Pr congener **15**, then to *t*Bu congener **16** and cHexyl congener **17**. The combined effect of tail branching and bulkiness in adamantyl congener **18** decreases the potency of the CAI relative to cHexyl congener **17** 1 order of magnitude for CA II (similarly to CA I) and 2 orders of magnitude for CA IV. Interestingly, adamantane derivative **18** retained nanomolar potency for CA IX, although about three times weaker than nPr congener **14**.

To provide a solid structural basis of the inhibitory profile of CAIs **13–18**, we undertook an extensive X-ray crystallographic study using the cytosolic CA II and the CA IX mimic.⁷⁰ The results are summarized in Figures 3–5. The 12 crystal structures were solved with high resolutions, ranging from 1.3 to 1.7 Å (Supporting Information Tables 1 and 2). The inhibitors bound as expected within active sites of both CA II and CA IX, anchoring their sulfonamide moiety through the catalytic zinc. All compounds displayed full electron density including tail atoms as seen in Figure 3. While examining these figures, one can observe that the tail of inhibitors **13–18** resides only in the hydrophobic pocket P1 in the case of the CA IX.

As seen in Figure 4B,I, compound **13** binds in a similar fashion in both CA isoforms with the exception of the final methyl group on the tail portion. In CAII, the methyl tail is positioned away from the bulky F131 and resides in pocket P2. In contrast, in CA IX, the methyl tail of compound **13** binds in pocket P1 adjacent to residue 131. Mention must be made that P1 pocket is larger in CA IX as compared with CA II, having a Val instead of a Phe in position 131, and therefore can accommodate easily hydrophobic tails of increased steric bulk, from Et (congener **13**) to adamantyl (congener **18**). The location of the hydrophobic tail of compounds **13–18**, in the large, hydrophobic pocket P1 of CA IX explains the constant nanomolar potency of these compounds against this target despite the significant increase in steric bulk and lipophilicity (log *P*'s between 0.8 and 2.28, Table 1). Even the bulkiest adamantyl derivative **18** can be fully accommodated in the P1 of CA IX, which explains why this derivative is most potent against CA IX. The pattern displayed by compound **13** binding in CA IX is repeated with the rest of the compounds, as seen in Figure 4C–G.

In contrast, in the case of CA II isozyme, the hydrophobic tail of compounds **13–18** was found to be located mostly in P2, opposite with the case of parent acetazolamide AAZ **1** that has the methyl located in the P1 pocket,^{59,71} thus revealing the importance of the tail approach also used in this study (Figure 4J–N). Interestingly, the only CAI that had the tail located outside the P2 pocket of CA II was the *t*Bu derivative **16**. In this case, the *t*Bu moiety is in fact located in between P1 and P2 pockets, displacing gently the Phe131 residue that normally separates the P1 and P2 pockets in CA II from its normal position (Figures 3–5). This translates into a slight decrease of potency relative to congeners **15** and **17** (Table 1). Compounds **13–17** each had higher specificity toward CA II over CA IX. With their smaller, nonbulky tails, these inhibitors were able to bind in the P2 pocket of CA II, resulting in stable and high-affinity binding. On the contrary, in CA IX, these inhibitors' tails went to the less sterically hindered P1 pocket binding near Val131 (Figure 3). However, with the addition of a bulky adamantyl group to the tail, steric clashes start to interfere with P2 pocket binding, thus specificity toward CA II drops. On the contrary, in CA IX, the adamantyl group can still bind with relatively high affinity to the less bulky P1 pocket of CA IX (Figure 3).

CONCLUSIONS

A detailed structure–activity relationship study was carried out within a series of lipophilic CAI with acetazolamide backbone **13–18**. The CAIs were profiled against the tumor-overexpressed CA IX, against ubiquitous cytosolic CA I and CA II and against membrane-bound CA IV. We identified several low

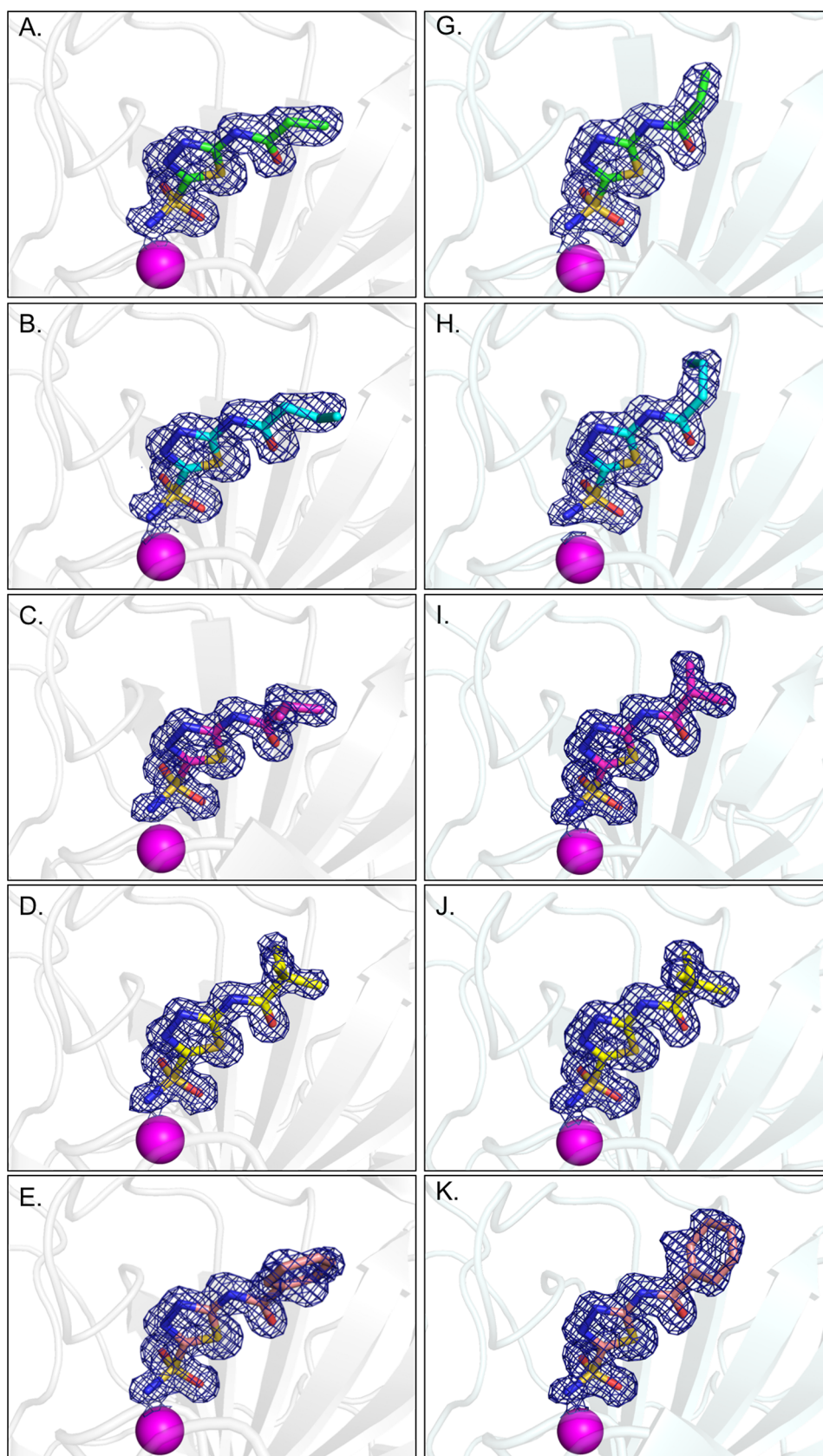


Figure 3. continued

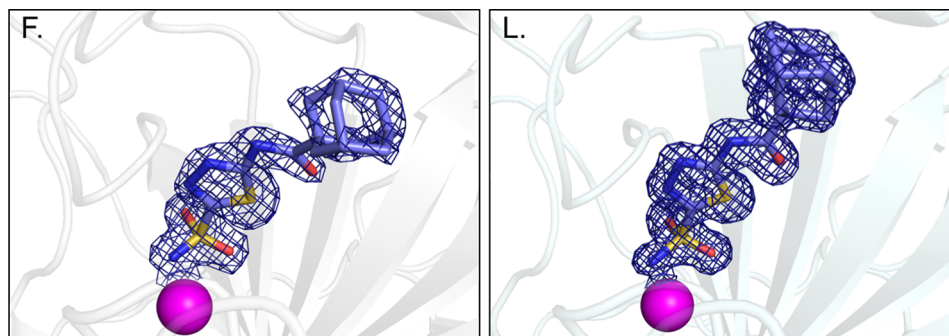


Figure 3. CA Inhibitors 13–18 electron density. Panels (A–F) are CA II and (G–L) are CA IX mimic complexes. CA II complex with (A) CAI 13 green, (B) CAI 14 blue, (C) CAI 15 pink, (D) CAI 16 yellow, (E) CAI 17 peach, and (F) CAI 18 purple. CA IX complex with (G) CAI 13 green, (H) CAI 14 blue, (I) CAI 15 pink, (J) CAI 16 yellow, (K) CAI 17 peach, and (L) CAI 18 purple. The 2FO-FC electron density maps (blue mesh) for each of the inhibitors are contoured to 1.0σ . Active site zinc is depicted as a magenta sphere.

nanomolar potent inhibitors against CA IX, with lipophilicities spanning two log units. We also identified very potent pan inhibitors such as **14**, with nanomolar potency against CA IX and sub-nanomolar potency against CA II and CA IV, and a good inhibition profile (1 order of magnitude) better than parent acetazolamide **1** against CA I. The adamantane derivative **18** displayed high potency against CA IX and CA II, involved in tumor pH homeostasis (Figure 1) and selectivity against membrane-bound CA IV, features that recommend this compound for translation to *in vivo* studies for the treatment of hypoxic solid tumors. We revealed the structural basis of these particular inhibition profiles through a comprehensive X-ray crystallographic study involving both CA II and CA IX comparatively, thus laying the basis for further developments toward more potent and selective inhibitors for the tumor-overexpressed CA IX isozyme.

EXPERIMENTAL SECTION

Materials. The following materials were used as received: propionic anhydride, butyric anhydride isobutyric anhydride (TCI America, Portland, OR), acetazolamide, pivaloyl chloride, cyclohexane carboxylic acid, adamantane carboxylic acid (Sigma, St Louis, MO); other salts, acids, and solvents (HPLC quality) were purchased from Fisher Scientific (Pittsburgh, PA), EMD (Gibbstown, NJ), and VWR International (West Chester, PA), respectively.

Techniques. The purity and the structure identity of the intermediary and the final products were assessed by a combination of techniques that included thin-layer chromatography (TLC), HPLC-MS, ^1H NMR, COSY, and ^{13}C NMR, high-resolution mass spectrometry (HR-MS). TLC was carried out on SiO_2 -precoated aluminum plates (silica gel with F254 indicator); layer thickness 200 μm ; pore size 60 \AA , from Sigma-Aldrich. Melting points were determined using a Thermolyne heating stage microscope (Dubuque, IA), equipped with an Olympus 5X objective, at heating/cooling rate of ~ 4 $^\circ\text{C}/\text{min}$ and were uncorrected. The purity of compounds was assessed *via* liquid chromatography-mass spectrometry (LC-MS) using an Agilent 1200 HPLC-DAD-MS system equipped with a G1315A DAD and a 6130 Quadrupole MS using a ZORBAX SB-C18 column, eluted with H_2O (0.1% HCOOH)/ MeCN (0.1% HCOOH) 95/5 to 0/100 linear gradient. NMR spectra were recorded at ≈ 300 K with a Bruker Avance III 400 Plus spectrometer equipped with a 5 mm indirect detection probe, operating at 400 MHz for ^1H NMR, at 100 MHz for ^{13}C NMR. Chemical shifts are reported as δ values, using tetramethylsilane (TMS) as an internal standard for proton spectra and the solvent resonance for carbon spectra. Assignments were made based on chemical shifts, signal intensity, COSY, HMQC, and HMBC sequences. For ^1H NMR, data are reported as follows: chemical shift, multiplicity (s = singlet, d = doublet, t = triplet, sep = septet, m = multiplet), coupling constants J (Hz), and integration.

Synthesis of 5-Amino-1,3,4-thiadiazole-2-sulfonamide (2). 5-Amino-1,3,4-thiadiazole-2-sulfonamide **2** was synthesized by deprotection of acetazolamide as previously described.^{34,72}

General Procedure for the Synthesis of Acyl Derivatives 13–16 (Method A). In a 100 mL round-bottom flask, 5-amino-1,3,4-thiadiazole-2-sulfonamide **2** (1.8 g, 10 mmol) was suspended in dry acetonitrile (30 mL) and cooled to 0 – 5 $^\circ\text{C}$ using an ice bath. The corresponding anhydride (12 mmol) was added dropwise to the cold suspension, under stirring. The ice bath was removed and the reaction mixture was stirred at room temperature for another 30 min, followed by heating it to reflux (TLC control, $\text{MeOH}/\text{CH}_2\text{Cl}_2$ 20/80 v/v). After all amine was consumed (1–3 h reflux), the reaction mixture was cooled and the solvent was evaporated to a small volume using a rotary evaporator when the product precipitates. The crude product was filtered out, washed with cold acetonitrile, and dried under vacuum. Recrystallization from alcohols (MeOH , EtOH) usually yielded the pure product, as evidenced by LC-MS (>96%). When purity was not satisfactory, flash chromatography was performed using $\text{MeOH}/\text{CH}_2\text{Cl}_2$ gradients. The pure fractions (by TLC) were grouped, evaporated to dryness, and crystallized from MeOH or EtOH . Reaction advancement was checked by TLC, and its completion was confirmed by LC-MS.

***N*-(5-Sulfamoyl-1,3,4-thiadiazol-2-yl)propionamide (13).** Mp 249 – 252 $^\circ\text{C}$ (lit³³ mp 147 – 148 $^\circ\text{C}$, lit⁷³ mp 247 – 248 $^\circ\text{C}$); yield 85.2%; ^1H NMR ($\text{DMSO}-d_6$, δ , ppm): 12.96 (s, 1H, $-\text{CONH}$), 8.32 (s, 2H, $-\text{SO}_2\text{NH}_2$), 2.54 (q, $J = 7.5$ Hz, 2H, CH_2CONH), and 1.13 (t, $J = 7.5$ Hz, 3H, $\text{CH}_3\text{CH}_2\text{CONH}$); ^{13}C NMR ($\text{DMSO}-d_6$, δ , ppm): 172.9 ($-\text{CONH}$), 164.2 (C5 TDA), 161.1 (C2, TDA), 28.2 ($-\text{CH}_2\text{CONH}$), and 8.7 ($\text{CH}_3\text{CH}_2\text{CONH}$); LC-MS: $\text{C}_5\text{H}_8\text{N}_4\text{O}_3\text{S}_2$, exact mass: 236.0; found: 237.0 (MH^+).

***N*-(5-Sulfamoyl-1,3,4-thiadiazol-2-yl)butyramide (14).** Mp 276 – 280 $^\circ\text{C}$ (lit³³ mp 260 – 262 $^\circ\text{C}$); yield 81.5%; ^1H NMR ($\text{DMSO}-d_6$, δ , ppm): 12.99 (s, 1H, $-\text{CONH}$), 8.32 (s, 2H, $-\text{SO}_2\text{NH}_2$), 2.53 (m, 2H, CH_2CONH), and 1.65 (sext, $J = 7.4$ Hz, 3H, $\text{CH}_3\text{CH}_2\text{CH}_2\text{CONH}$); 0.90 (t, $J = 7.4$ Hz, 3H, $\text{CH}_3\text{CH}_2\text{CH}_2\text{CONH}$); ^{13}C NMR ($\text{DMSO}-d_6$, δ , ppm): 172.1 ($-\text{CONH}$), 164.2 (C5 TDA), 161.0 (C2, TDA), 36.6 ($-\text{CH}_2\text{CONH}$), 17.8 ($-\text{CH}_2\text{CH}_2\text{CONH}$), and 13.4 ($\text{CH}_3\text{CH}_2\text{CH}_2\text{CONH}$); LC-MS: $\text{C}_6\text{H}_{10}\text{N}_4\text{O}_3\text{S}_2$, exact mass: 250.0; found: 251.0 (MH^+).

***N*-(5-Sulfamoyl-1,3,4-thiadiazol-2-yl)isobutyramide (15).** Mp 281 – 283 $^\circ\text{C}$ (lit³³ mp 280 – 283 $^\circ\text{C}$); yield 79.2%; ^1H NMR ($\text{DMSO}-d_6$, δ , ppm): 12.98 (s, 1H, $-\text{CONH}$), 8.32 (s, 2H, $-\text{SO}_2\text{NH}_2$), 2.82 (hep, $J = 6.8$ Hz, 1H, CHCONH), and 1.15 (d, $J = 6.9$ Hz, 6H, $(\text{CH}_3)_2\text{CHCONH}$); ^{13}C NMR ($\text{DMSO}-d_6$, δ , ppm): 176.0 ($-\text{CONH}$), 164.3 (C5 TDA), 161.2 (C2, TDA), 33.9 ($-\text{CHCONH}$), and 18.8 ($(\text{CH}_3)_2\text{CHCONH}$); LC-MS: $\text{C}_6\text{H}_{10}\text{N}_4\text{O}_3\text{S}_2$, exact mass: 250.0; found: 251.0 (MH^+).

General Procedure for the Synthesis of Acyl Derivatives 17,18 (Method B). In a 100 mL round-bottom flask, 5-amino-1,3,4-thiadiazole-2-sulfonamide **2** (1.8 g, 10 mmol) was suspended in dry

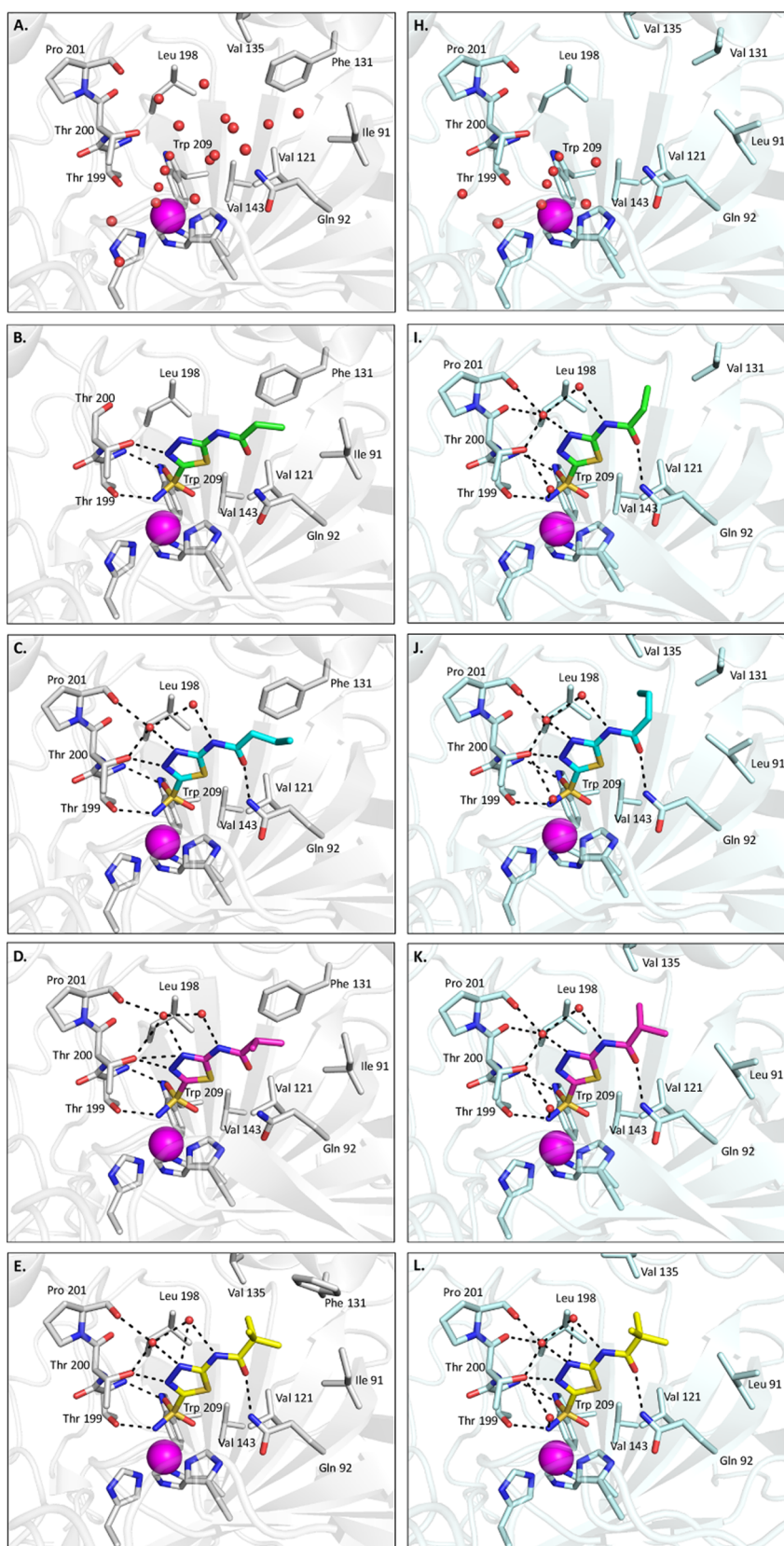


Figure 4. continued

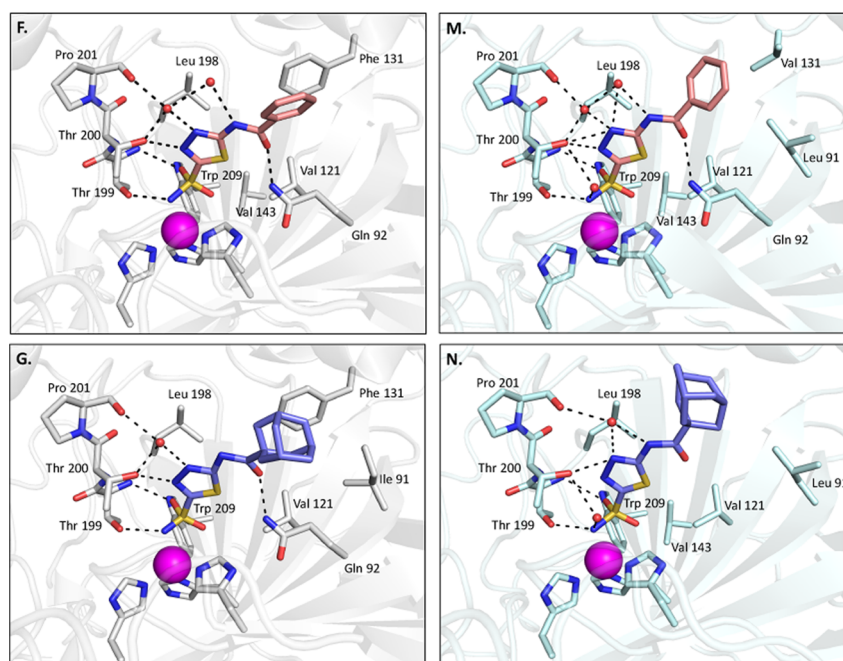


Figure 4. Interactions of inhibitors 13–18 with CA II and CA IX. Panels (A) and (H) are the unbound active sites of CA II (PDB 3KS3) and CA IX mimic (PDB 4ZAO), respectively. Panels (B–G) are CA II and panels (I–N) are CA IX mimic complexes. CA II complex with (B) CAI 13 green, (C) CAI 14 blue, (D) CAI 15 pink, (E) CAI 16 yellow, (F) CAI 17 peach, and (G) CAI 18 purple. CA IX complex with (I) CAI 13, (J) CAI 14 blue, (K) CAI 15 pink, (L) CAI 16 yellow, (M) CAI 17 peach, and (N) CAI 18 purple. Active site zinc is depicted as a magenta sphere, and active site histidines are represented by sticks. Ordered active site waters are represented by red spheres.

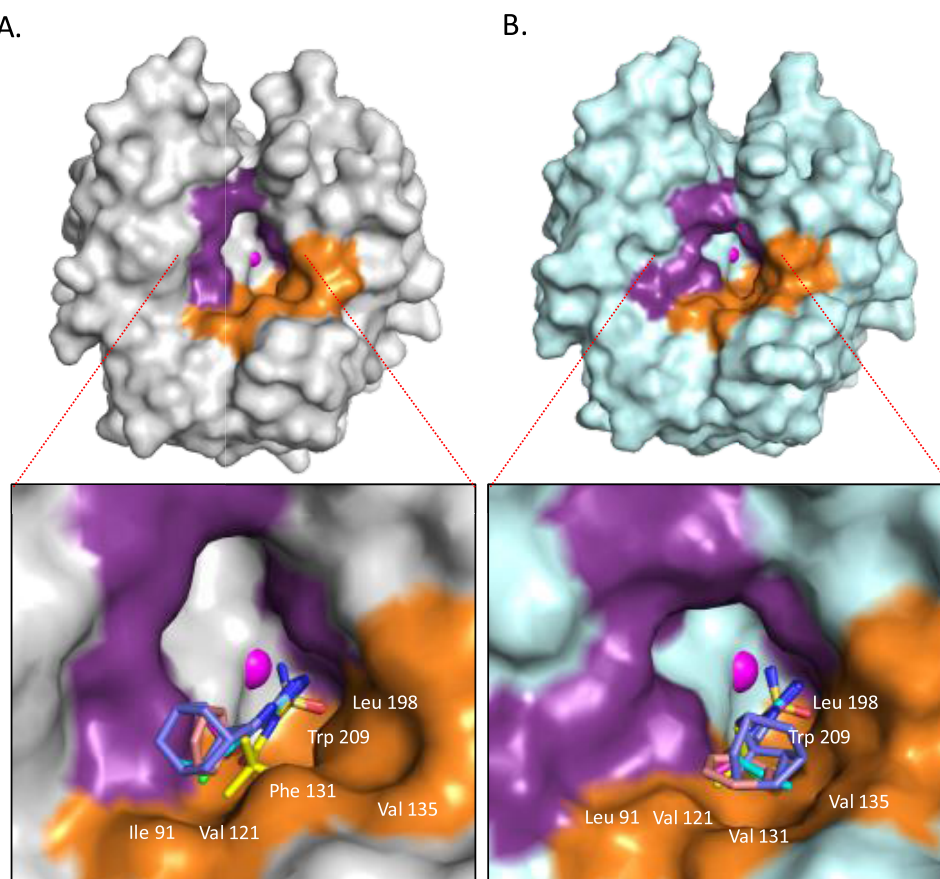


Figure 5. Superposition of CAIs 13–18 binding. Surface representation of (A) CA II and (B) CA IX mimic in complex with CAIs 13–18. CAI 13 green, CAI 14 blue, CAI 15 pink, CAI 16 yellow, CAI 17 peach, and CAI 18 purple. Note that residue 131 has a key role in the binding modes of the tails of the inhibitors in CA II and CA IX.

acetonitrile (20 mL), under stirring. Pyridine (0.95 g, 12 mmol) was added *via* a syringe and the reaction mixture was cooled to 0–5 °C using an ice bath. The corresponding acyl chloride (12 mmol, made from the corresponding acid with thionyl chloride), dissolved in 5–10 mL of dry acetonitrile, was added dropwise to the cold suspension, under stirring. Stirring was continued for 1 h when a white precipitate of pyridinium chloride was formed. The ice bath was removed and the reaction mixture was stirred at room temperature until completion (TLC control, MeOH/CH₂Cl₂ 20/80 v/v). The solvent was evaporated to dryness using a rotary evaporator and the residue was treated with 10 mL of DI water, stirred for 5 min, then filtered, and washed with cold DI water. Recrystallization from alcohols (MeOH, EtOH) usually yielded the pure product, as evidenced by LC-MS (>96%). When purity was not satisfactory, flash chromatography was performed using MeOH/CH₂Cl₂ gradients. The pure fractions (by TLC) were grouped, evaporated to dryness, and crystallized from MeOH or EtOH. Reaction advancement was checked by TLC and its completion was confirmed by LC-MS.

N-(5-Sulfamoyl-1,3,4-thiadiazol-2-yl)pivalamide (16). Mp 256–258 °C (lit⁷⁴ mp 252–254 °C); yield 82.1%; ¹H NMR (DMSO-*d*₆, δ, ppm): 12.73 (s, 1H, –CONH), 8.32 (s, 2H, –SO₂NH₂), and 1.28 (s, 9H, (CH₃)₃CCONH); ¹³C NMR (DMSO-*d*₆, δ, ppm): 177.4 (–CONH), 164.4 (C5 TDA), 161.9 (C2, TDA), 30.6 (–CCONH), and 26.3 (CH₃)₃CCONH; LC-MS: C₇H₁₂N₄O₃S₂, exact mass: 264.0; found: 265.0 (MH⁺).

N-(5-Sulfamoyl-1,3,4-thiadiazol-2-yl)cyclohexanecarboxamide (17). Mp 255–259 °C; yield 78.6%; ¹H NMR (DMSO-*d*₆, δ, ppm): 12.96 (s, 1H, –CONH), 8.32 (s, 2H, –SO₂NH₂), 2.55 (m, 1H, CHCONH), and 1.10–1.90 (m, 10H, cyclohexyl); ¹³C NMR (DMSO-*d*₆, δ, ppm): 175.0 (–CONH), 164.3 (C5 TDA), 161.2 (C2, TDA), 42.3 (CαCONH), 28.5 (2C, CβCONH), 25.1 (CδCONH), and 24.9 (2C, CγCONH); LC-MS: C₉H₁₄N₄O₃S₂, exact mass: 290.0; found: 291.0 (MH⁺); anal (C₉H₁₄N₄O₃S₂) C, H, N. Requires: C 37.23, H 4.86, N 19.30; found: C 37.20, H 4.95, N 19.36.

N-(5-Sulfamoyl-1,3,4-thiadiazol-2-yl)adamantanecarboxamide (18). Mp 246–248 °C (lit⁷⁵ mp 246–248 °C); yield 75.2%; ¹H NMR (DMSO-*d*₆, δ, ppm): 12.68 (s, 1H, –CONH), 8.31 (s, 2H, –SO₂NH₂), 1.82–2.10 (m, 9H, Ad), and 1.60–1.80 (m, 6H, Ad); ¹³C NMR (DMSO-*d*₆, δ, ppm): 176.7 (–CONH), 164.4 (C5 TDA), 161.9 (C2, TDA), 40.8 (CαCONH Ad), 37.3 (3C, CβCONH Ad), 35.6 (3C, CγCONH Ad), and 27.3 (3C, CδCONH Ad); LC-MS: C₁₃H₁₆N₄O₃S₂, exact mass: 340.0; found: 341.0 (MH⁺).

CA Inhibition Assay. An applied photophysics stopped-flow instrument has been used for assaying the CA-catalyzed CO₂ hydration activity.⁷⁶ Phenol red (at a concentration of 0.2 mM) has been used as an indicator, working at the absorbance maximum of 557 nm, with 20 mM Hepes (pH 7.5) as buffer, and 20 mM Na₂SO₄ (for maintaining constant the ionic strength), following the initial rates of the CA-catalyzed CO₂ hydration reaction for a period of 10–100 s. The CO₂ concentrations ranged from 1.7 to 17 mM for the determination of the kinetic parameters and inhibition constants. For each inhibitor, at least six traces of the initial 5–10% of the reaction have been used for determining the initial velocity. The uncatalyzed rates were determined in the same manner and subtracted from the total observed rates. Stock solutions of inhibitor (0.1 mM) were prepared in distilled-deionized water and dilutions up to 0.01 nM were done thereafter with the assay buffer. Inhibitor and enzyme solutions were preincubated together for 15 min at room temperature prior to assay to allow for the formation of the E–I complex. The inhibition constants were obtained by nonlinear least-squares methods using PRISM 3 and the Cheng–Prusoff equation, as reported earlier,³⁸ and represent the mean from at least three different determinations. All CA isoforms were recombinant ones obtained in-house as reported earlier.^{21,32,75,77}

Protein Expression and Purification. CA II and CA IX mimic were expressed and purified according to previously published protocols.⁷⁰ Briefly, the gene-containing plasmid was transformed into competent BL21 *Escherichia coli* cells *via* a standard BL21 transformation protocol. After growth in SOC media, the cultures

were transferred to an overnight growth in nutrient-rich Luria Broth. Cultures were then allowed to grow to an optical density of 0.6 at 600 nm in a 2 L culture flask in the presence of selecting antibiotic. The *E. coli* was then induced by the addition of 0.5 mM isopropyl β-D-1-thiogalactoside (IPTG) and 1 mM zinc sulfate and incubated for an additional 3 h. Cells were then lysed using a microfluidizer set to 18 000 psi and purified using affinity chromatography with a benzenesulfonamide resin. Purity was determined with SDS-Page and concentration was determined by UV–vis spectroscopy at 280 nm.

X-ray Crystallography. CAII and CA IX mimic were cocrystallized with a series of 6 CA inhibitors 3–8. Each crystallization drop was prepared by adding 4.5 μL of protein in a 1:1 ratio with 4.5 μL of the precipitant solution of 1.6 M sodium citrate and 50 mM Tris at a pH of 7.8 to a final volume of 9 μL. Inhibitor stock solutions of varying concentrations were made in dimethyl sulfoxide (DMSO) to determine solubility. Approximately, 1 μL of 200 mM of each inhibitor was added to the crystallization drop to a final volume of 10 μL. Crystal trays were incubated at room temperature and undisturbed for 2 weeks until crystals formed. The complexes of CAI 8 could not be obtained *via* cocrystallization due to the high log *P* value of the inhibitor. Instead, the preformed crystals of CA II and CA IX mimic were soaked with ~80 mM CAI 8 in 10% DMSO. Data was collected at cryogenic temperatures at Cornell High Energy Synchrotron Source (CHESS) and Stanford Synchrotron Radiation Lightsource (SSRL), using a Pilatus 6M detector. The diffraction images were indexed, integrated, merged, and scaled to the P21 space group using XDS *via* the CCP4 program suite⁷⁸ The diffraction data was phased with standard Molecular replacement methods using the software package PHENIX with the PDB entry 3KS3 as the search model.^{79,80} Coordinate refinements and inhibitor restraints were calculated using PHENIX.⁷⁹ The program Coot was utilized in between refinements to add a solvent and inhibitor molecules and make individual real space refinements of each residue when needed.⁸¹ Figures were generated in the molecular graphical software PyMol (Schrodinger LLC), and protein–ligand interactions and bond lengths were determined using LigPlot Plus.⁸² The inhibitor surface interactions were determined using online server PDB Pisa.⁸³

■ ASSOCIATED CONTENT

Supporting Information

The Supporting Information is available free of charge at <https://pubs.acs.org/doi/10.1021/acs.jmedchem.0c01390>.

Crystallographic CA II complex structure statistics; and crystallographic CA IX_{mimic}-complex structure statistics (PDF)

HPLC traces of investigated compounds (PDF)

Smiles (CSV)

■ AUTHOR INFORMATION

Corresponding Authors

Claudio T. Supuran – NEUROFARBA Department, Pharmaceutical Sciences Section, Università degli Studi di Firenze, 50019 Sesto Fiorentino, Florence, Italy; orcid.org/0000-0003-4262-0323; Phone: 39-055-4573005; Email: claudio.supuran@unifi.it; Fax: 39-055-4573385

Marc A. Ilies – Department of Pharmaceutical Sciences and Moulder Center for Drug Discovery Research, Temple University School of Pharmacy, Philadelphia, Pennsylvania 19140, United States; orcid.org/0000-0003-0694-411X; Phone: 215-707-1749; Email: mailies@temple.edu; Fax: 215-707-5620

Robert McKenna – Department of Biochemistry and Molecular Biology, College of Medicine, University of Florida, Gainesville, Florida 32610, United States; Phone: (352) 294-8395; Email: rmckenna@ufl.edu

Authors

Jacob T. Andring – Department of Biochemistry and Molecular Biology, College of Medicine, University of Florida, Gainesville, Florida 32610, United States; orcid.org/0000-0002-6632-6391

Mallorie Fouch – Department of Pharmaceutical Sciences and Moulder Center for Drug Discovery Research, Temple University School of Pharmacy, Philadelphia, Pennsylvania 19140, United States

Suleyman Akocak – Department of Pharmaceutical Sciences and Moulder Center for Drug Discovery Research, Temple University School of Pharmacy, Philadelphia, Pennsylvania 19140, United States

Andrea Angeli – NEUROFARBA Department, Pharmaceutical Sciences Section, Università degli Studi di Firenze, 50019 Sesto Fiorentino, Florence, Italy; orcid.org/0000-0002-1470-7192

Complete contact information is available at:

<https://pubs.acs.org/10.1021/acs.jmedchem.0c01390>

Author Contributions

The manuscript was written through the contributions of all authors. All authors have given approval to the final version of the manuscript.

Notes

The authors declare no competing financial interest.

ACKNOWLEDGMENTS

We would like to thank the staff, operators, and scientists at SSRL and CHESS for their assistance in X-ray crystallography data acquisition. MAI acknowledges the financial support of NIH (Grant R03EB026189) and of Edward N. & Della Thome Memorial Foundation. Suleyman Akocak acknowledges the financial support of the Turkish Minister of Education for a PhD scholarship. The support of Temple Undergraduate Research Program is also gratefully acknowledged.

ABBREVIATIONS

CA, carbonic anhydrase; CAI, carbonic anhydrase inhibitor; HIF-1, hypoxia-inducible factor 1; ATP, adenosine triphosphate; AAZ, acetazolamide; MZA, methazolamide; EZA, ethoxzolamide; BZA, benzolamide; DCP, dichlorphenamide; IPTG, isopropyl β -D-1-thiogalactoside; CHESS, Cornell High Energy Synchrotron Source; SSRL, Stanford Synchrotron Radiation Lightsource

REFERENCES

- (1) Semenza, G. L. Hypoxia-inducible factors: mediators of cancer progression and targets for cancer therapy. *Trends Pharmacol. Sci.* **2012**, *33*, 207–214.
- (2) Semenza, G. L. Targeting HIF-1 for cancer therapy. *Nat. Rev. Cancer* **2003**, *3*, 721–732.
- (3) Supuran, C. T. Carbonic anhydrases: novel therapeutic applications for inhibitors and activators. *Nat. Rev. Drug Discovery* **2008**, *7*, 168–181.
- (4) Neri, D.; Supuran, C. T. Interfering with pH regulation in tumours as a therapeutic strategy. *Nat. Rev. Drug Discovery* **2011**, *10*, 767–777.
- (5) Alterio, V.; Di Fiore, A.; D'Ambrosio, K.; Supuran, C. T.; De Simone, G. Multiple binding modes of inhibitors to carbonic anhydrases: how to design specific drugs targeting 15 different isoforms? *Chem. Rev.* **2012**, *112*, 4421–4468.

(6) Pastorek, J.; Pastorekova, S.; Callebaut, I.; Mornon, J. P.; Zelnik, V.; Opavsky, R.; Zat'ovicova, M.; Liao, S.; Portetelle, D.; Stanbridge, E. J. Cloning and characterization of MN, a human tumor-associated protein with a domain homologous to carbonic anhydrase and a putative helix-loop-helix DNA binding segment. *Oncogene* **1994**, *9*, 2877–2888.

(7) Alterio, V.; Hilvo, M.; Di Fiore, A.; Supuran, C. T.; Pan, P.; Parkkila, S.; Scaloni, A.; Pastorek, J.; Pastorekova, S.; Pedone, C.; Scozzafava, A.; Monti, S. M.; De Simone, G. Crystal structure of the catalytic domain of the tumor-associated human carbonic anhydrase IX. *Proc. Natl. Acad. Sci. U.S.A.* **2009**, *106*, 16233–16238.

(8) Tureci, O.; Sahin, U.; Vollmar, E.; Siemer, S.; Gottert, E.; Seitz, G.; Parkkila, A. K.; Shah, G. N.; Grubb, J. H.; Pfreundschuh, M.; Sly, W. S. Human carbonic anhydrase XII: cDNA cloning, expression, and chromosomal localization of a carbonic anhydrase gene that is overexpressed in some renal cell cancers. *Proc. Natl. Acad. Sci. U.S.A.* **1998**, *95*, 7608–7613.

(9) Whittington, D. A.; Waheed, A.; Ulmasov, B.; Shah, G. N.; Grubb, J. H.; Sly, W. S.; Christianson, D. W. Crystal structure of the dimeric extracellular domain of human carbonic anhydrase XII, a dimeric membrane protein overexpressed in certain cancer tumor cells. *Proc. Natl. Acad. Sci. U.S.A.* **2001**, *98*, 9545–9550.

(10) Shabana, A. M.; Ilies, M. A. Drug delivery to hypoxic tumors targeting carbonic anhydrase ix, in targeted nanosystems for therapeutic applications: new concepts, dynamic properties, efficiency, and toxicity. *Am. Chem. Soc.* **2019**, 223–252.

(11) Zamanova, S.; Shabana, A. M.; Mondal, U. K.; Ilies, M. A. Carbonic anhydrases as disease markers. *Expert Opin. Ther. Pat.* **2019**, *29*, 509–533.

(12) Austin, R. P.; Barton, P.; Cockroft, S. L.; Wenlock, M. C.; Riley, R. J. The influence of nonspecific microsomal binding on apparent intrinsic clearance, and its prediction from physicochemical properties. *Drug Metab. Dispos.* **2002**, *30*, 1497–1503.

(13) Pastoreková, S.; Pastorek, J. Cancer-related carbonic anhydrase isozymes and their inhibition. *Carbonic Anhydrase* **2004**, 255–281.

(14) Saarnio, J.; Parkkila, S.; Parkkila, A. K.; Haukipuro, K.; Pastorekova, S.; Pastorek, J.; Kairaluoma, M. I.; Karttunen, T. J. Immunohistochemical study of colorectal tumors for expression of a novel transmembrane carbonic anhydrase, MN/CA IX, with potential value as a marker of cell proliferation. *Am. J. Pathol.* **1998**, *153*, 279–285.

(15) Swietach, P.; Wigfield, S.; Cobden, P.; Supuran, C. T.; Harris, A. L.; Vaughan-Jones, R. D. Tumor-associated carbonic anhydrase 9 spatially coordinates intracellular pH in three-dimensional multicellular growths. *J. Biol. Chem.* **2008**, *283*, 20473–20483.

(16) Gatenby, R. A.; Gawlinski, E. T.; Gmitro, A. F.; Kaylor, B.; Gillies, R. J. Acid-mediated tumor invasion: a multidisciplinary study. *Cancer Res.* **2006**, *66*, 5216–5223.

(17) Gatenby, R. A.; Gillies, R. J. Why do cancers have high aerobic glycolysis? *Nat. Rev. Cancer* **2004**, *4*, 891–899.

(18) Švastová, E.; Hulikova, A.; Rafajova, M.; Zat'ovicova, M.; Gibadulinova, A.; Casini, A.; Cecchi, A.; Scozzafava, A.; Supuran, C. T.; Pastorek, J.; Pastorekova, S. Hypoxia activates the capacity of tumor-associated carbonic anhydrase IX to acidify extracellular pH. *FEBS Lett.* **2004**, *577*, 439–445.

(19) Ennaceur, A. One-trial object recognition in rats and mice: methodological and theoretical issues. *Behav. Brain Res.* **2010**, *215*, 244–254.

(20) Arqué, G.; Fotaki, V.; Fernandez, D.; Martinez de Lagran, M.; Arbones, M. L.; Dierssen, M. Impaired spatial learning strategies and novel object recognition in mice haploinsufficient for the dual specificity tyrosine-regulated kinase-1A (Dyrk1A). *PLoS One* **2008**, *3*, No. e2575.

(21) Dave, K.; Scozzafava, A.; Vullo, D.; Supuran, C. T.; Ilies, M. A. Pyridinium derivatives of histamine are potent activators of cytosolic carbonic anhydrase isoforms I, II and VII. *Org. Biomol. Chem.* **2011**, *9*, 2790–2800.

(22) Chen, C. L.; Chu, J. S.; Su, W. C.; Huang, S. C.; Lee, W. Y. Hypoxia and metabolic phenotypes during breast carcinogenesis:

expression of HIF-1 α , GLUT1, and CAIX. *Virchows Arch.* **2010**, *457*, 53–61.

(23) Choschzick, M.; Oosterwijk, E.; Muller, V.; Woelber, L.; Simon, R.; Moch, H.; Tennstedt, P. Overexpression of carbonic anhydrase IX (CAIX) is an independent unfavorable prognostic marker in endometrioid ovarian cancer. *Virchows Arch.* **2011**, *459*, 193–200.

(24) Hynninen, P.; Vaskivuo, L.; Saarnio, J.; Haapasalo, H.; Kivela, J.; Pastorekova, S.; Pastorek, J.; Waheed, A.; Sly, W. S.; Puistola, U.; Parkkila, S. Expression of transmembrane carbonic anhydrases IX and XII in ovarian tumours. *Histopathology* **2006**, *49*, 594–602.

(25) Dave, K.; Ilies, M. A.; Scozzafava, A.; Temperini, C.; Vullo, D.; Supuran, C. T. An inhibitor-like binding mode of a carbonic anhydrase activator within the active site of isoform II. *Bioorg. Med. Chem. Lett.* **2011**, *21*, 2764–2768.

(26) Koukourakis, M. I.; Bentzen, S. M.; Giatromanolaki, A.; Wilson, G. D.; Daley, F. M.; Saunders, M. I.; Dische, S.; Sivridis, E.; Harris, A. L. Endogenous markers of two separate hypoxia response pathways (hypoxia inducible factor 2 α and carbonic anhydrase 9) are associated with radiotherapy failure in head and neck cancer patients recruited in the CHART randomized trial. *J. Clin. Oncol.* **2006**, *24*, 727–735.

(27) Barker, P. L.; Gendler, P. L.; Rapoport, H. Acylation of dibasic compounds containing amino amidine and aminoguanidine functions. *J. Org. Chem.* **1981**, *46*, 2455–2465.

(28) Ganti, V.; Walker, E. A.; Nagar, S. Pharmacokinetic application of a bio-analytical LC-MS method developed for 5-fluorouracil and methotrexate in mouse plasma, brain and urine. *Biomed. Chromatogr.* **2013**, *27*, 994–1002.

(29) Bisen-Hersh, E. B.; Hinehline, P. N.; Walker, E. A. Effects of early chemotherapeutic treatment on learning in adolescent mice: implications for cognitive impairment and remediation in childhood cancer survivors. *Clin. Cancer Res.* **2013**, *19*, 3008–3018.

(30) Hussain, S. A.; Palmer, D. H.; Ganesan, R.; Hiller, L.; Gregory, J.; Murray, P. G.; Pastorek, J.; Young, L.; James, N. D. Carbonic anhydrase IX, a marker of hypoxia: correlation with clinical outcome in transitional cell carcinoma of the bladder. *Oncol. Rep.* **2004**, *11*, 1005–1010.

(31) Bushnell, P. J. Advanced behavioral testing in rodents: assessment of cognitive function in animals. *Curr. Protoc. Toxicol.* **2001**, *11.4.1*–*11.4.34*.

(32) Ilies, M. A.; Vullo, D.; Pastorek, J.; Scozzafava, A.; Ilies, M.; Caproui, M. T.; Pastorekova, S.; Supuran, C. T. Carbonic anhydrase inhibitors. Inhibition of tumor-associated isozyme IX by halogen-sulfanilamide and halogenophenylaminobenzolamide derivatives. *J. Med. Chem.* **2003**, *46*, 2187–2196.

(33) Vaughan, J. R., Jr.; Eichler, J. A.; Anderson, G. W. Notes - Heterocyclic sulfonamides as carbonic Anhydrase inhibitors. 2-Acylamido- and 2-sulfonamido-1,3,4-thiadiazole-5-sulfonamides. *J. Inorg. Chem.* **1956**, *21*, 700–701.

(34) Supuran, C. T.; Ilies, M. A.; Scozzafava, A. Carbonic anhydrase inhibitors - Part 29: Interaction of isozymes I, II and IV with benzolamide-like derivatives. *Eur. J. Med. Chem.* **1998**, *33*, 739–751.

(35) Supuran, C. T.; Scozzafava, A.; Ilies, M. A.; Iorga, B.; Cristea, T.; Briganti, F.; Chiraleu, F.; Banciu, M. D. Carbonic anhydrase inhibitors - Part 53 - Synthesis of substituted-pyridinium derivatives of aromatic sulfonamides: The first non-polymeric membrane-impermeable inhibitors with selectivity for isozyme IV. *Eur. J. Med. Chem.* **1998**, *33*, 577–594.

(36) Supuran, C. T.; Scozzafava, A.; Jurca, B.; Ilies, M. A. Carbonic anhydrase inhibitors - Part 49: Synthesis of substituted ureido and thioureido derivatives of aromatic/heterocyclic sulfonamides with increased affinities for isozyme I. *Eur. J. Med. Chem.* **1998**, *33*, 83–93.

(37) Scozzafava, A.; Briganti, F.; Ilies, M. A.; Supuran, C. T. Carbonic anhydrase inhibitors: synthesis of membrane-impermeant low molecular weight sulfonamides possessing in vivo selectivity for the membrane-bound versus cytosolic isozymes. *J. Med. Chem.* **2000**, *43*, 292–300.

(38) Casini, A.; Scozzafava, A.; Mincione, F.; Menabuoni, L.; Ilies, M. A.; Supuran, C. T. Carbonic anhydrase inhibitors: water-soluble 4-

sulfamoylphenylthioureas as topical intraocular pressure-lowering agents with long-lasting effects. *J. Med. Chem.* **2000**, *43*, 4884–4892.

(39) McKenna, R.; Supuran, C. T. Carbonic anhydrase inhibitors drug design. *Subcell. Biochem.* **2014**, *75*, 291–323.

(40) Pacchiano, F.; Carta, F.; McDonald, P. C.; Lou, Y.; Vullo, D.; Scozzafava, A.; Dedhar, S.; Supuran, C. T. Ureido-substituted benzenesulfonamides potently inhibit carbonic anhydrase IX and show antimetastatic activity in a model of breast cancer metastasis. *J. Med. Chem.* **2011**, *54*, 1896–1902.

(41) Supuran, C. T.; Scozzafava, A.; Ilies, M. A.; Briganti, F. Carbonic anhydrase inhibitors: synthesis of sulfonamides incorporating 2,4,6-trisubstituted-pyridinium-ethylcarboxamido moieties possessing membrane-impermeability and in vivo selectivity for the membrane-bound (CA IV) versus the cytosolic (CA I and CA II) isozymes. *J. Enzyme Inhib.* **2000**, *15*, 381–401.

(42) Casey, J. R.; Morgan, P. E.; Vullo, D.; Scozzafava, A.; Mastrolorenzo, A.; Supuran, C. T. Carbonic anhydrase inhibitors. Design of selective, membrane-impermeant inhibitors targeting the human tumor-associated isozyme IX. *J. Med. Chem.* **2004**, *47*, 2337–2347.

(43) Winum, J. Y.; Casini, A.; Mincione, F.; Starnotti, M.; Montero, J. L.; Scozzafava, A.; Supuran, C. T. Carbonic anhydrase inhibitors: N-(p-sulfamoylphenyl)- α -D-glycopyranosylamines as topically acting antiglaucoma agents in hypertensive rabbits. *Bioorg. Med. Chem. Lett.* **2004**, *14*, 225–229.

(44) Wilkinson, B. L.; Bornaghi, L. F.; Houston, T. A.; Innocenti, A.; Supuran, C. T.; Poulsen, S. A. A novel class of carbonic anhydrase inhibitors: glycoconjugate benzene sulfonamides prepared by “click-tailing”. *J. Med. Chem.* **2006**, *49*, 6539–6548.

(45) Morris, J. C.; Chiche, J.; Grellier, C.; Lopez, M.; Bornaghi, L. F.; Maresca, A.; Supuran, C. T.; Pouyssegur, J.; Poulsen, S. A. Targeting hypoxic tumor cell viability with carbohydrate-based carbonic anhydrase IX and XII inhibitors. *J. Med. Chem.* **2011**, *54*, 6905–6918.

(46) Tanpure, R. P.; Ren, B.; Peat, T. S.; Bornaghi, L. F.; Vullo, D.; Supuran, C. T.; Poulsen, S. A. Carbonic anhydrase inhibitors with dual-tail moieties to match the hydrophobic and hydrophilic halves of the carbonic anhydrase active site. *J. Med. Chem.* **2015**, *58*, 1494–1501.

(47) Winum, J. Y.; Colinas, P. A.; Supuran, C. T. Glycosidic carbonic anhydrase IX inhibitors: a sweet approach against cancer. *Bioorg. Med. Chem.* **2013**, *21*, 1419–1426.

(48) Akocak, S.; Alam, M. R.; Shabana, A. M.; Sanku, R. K. K.; Vullo, D.; Thompson, H.; Swenson, E. R.; Supuran, C. T.; Ilies, M. A. Pegylated bis-sulfonamide carbonic anhydrase inhibitors can efficiently control the growth of several carbonic anhydrase ix-expressing carcinomas. *J. Med. Chem.* **2016**, *59*, 5077–5088.

(49) Supuran, C. T.; Winum, J. Y. Carbonic anhydrase IX inhibitors in cancer therapy: an update. *Future Med. Chem.* **2015**, *7*, 1407–1414.

(50) Mboge, M. Y.; Mahon, B. P.; McKenna, R.; Frost, S. C. Carbonic Anhydrases: Role in pH Control and Cancer. *Metabolites* **2018**, *8*, 19.

(51) Mahon, B. P.; Pinard, M. A.; McKenna, R. Targeting carbonic anhydrase IX activity and expression. *Molecules* **2015**, *20*, 2323–2348.

(52) Lou, Y.; McDonald, P. C.; Oloumi, A.; Chia, S.; Ostlund, C.; Ahmadi, A.; Kyle, A.; Auf dem Keller, U.; Leung, S.; Huntsman, D.; Clarke, B.; Sutherland, B. W.; Waterhouse, D.; Bally, M.; Roskelley, C.; Overall, C. M.; Minchinton, A.; Pacchiano, F.; Carta, F.; Scozzafava, A.; Touisni, N.; Winum, J. Y.; Supuran, C. T.; Dedhar, S. Targeting tumor hypoxia: suppression of breast tumor growth and metastasis by novel carbonic anhydrase IX inhibitors. *Cancer Res.* **2011**, *71*, 3364–3376.

(53) McDonald, P. C.; Winum, J. Y.; Supuran, C. T.; Dedhar, S. Recent developments in targeting carbonic anhydrase IX for cancer therapeutics. *Oncotarget* **2012**, *3*, 84–97.

(54) Pacchiano, F.; Aggarwal, M.; Avvaru, B. S.; Robbins, A. H.; Scozzafava, A.; McKenna, R.; Supuran, C. T. Selective hydrophobic pocket binding observed within the carbonic anhydrase II active site accommodate different 4-substituted-ureido-benzenesulfonamides

and correlate to inhibitor potency. *Chem. Commun.* **2010**, *46*, 8371–8373.

(55) Akocak, S.; Ilies, M. A. Next-Generation Primary Sulfonamide Carbonic Anhydrase Inhibitors. In *Targeting Carbonic Anhydrases*; Future Science: London, 2014; pp 35–51.

(56) Supuran, C. T.; Winum, J. Y. Designing carbonic anhydrase inhibitors for the treatment of breast cancer. *Expert Opin. Drug Discovery* **2015**, *10*, 591–597.

(57) Akocak, S.; Lolak, N.; Bua, S.; Supuran, C. T. Discovery of novel 1,3-diaryltriazene sulfonamides as carbonic anhydrase I, II, VII, and IX inhibitors. *J. Enzyme Inhib. Med. Chem.* **2018**, *33*, 1575–1580.

(58) Menchise, V.; De Simone, G.; Di Fiore, A.; Scozzafava, A.; Supuran, C. T. Carbonic anhydrase inhibitors: X-ray crystallographic studies for the binding of 5-amino-1,3,4-thiadiazole-2-sulfonamide and 5-(4-amino-3-chloro-5-fluorophenylsulfonamido)-1,3,4-thiadiazole-2-sulfonamide to human isoform II. *Bioorg. Med. Chem. Lett.* **2006**, *16*, 6204–6208.

(59) Sippel, K. H.; Robbins, A. H.; Domsic, J.; Genis, C.; Agbandje-McKenna, M.; McKenna, R. High-resolution structure of human carbonic anhydrase II complexed with acetazolamide reveals insights into inhibitor drug design. *Acta Crystallogr., Sect. F: Struct. Biol. Cryst. Commun.* **2009**, *65*, 992–995.

(60) Lomelino, C. L.; Andring, J. T.; McKenna, R. Crystallography and its impact on carbonic anhydrase research. *Int. J. Med. Chem.* **2018**, *2018*, No. 9419521.

(61) Lomelino, C. L.; Mahon, B. P.; McKenna, R.; Carta, F.; Supuran, C. T. Kinetic and X-ray crystallographic investigations on carbonic anhydrase isoforms I, II, IX and XII of a thioureido analog of SLC-0111. *Bioorg. Med. Chem.* **2016**, *24*, 976–981.

(62) Menchise, V.; De Simone, G.; Alterio, V.; Di Fiore, A.; Pedone, C.; Scozzafava, A.; Supuran, C. T. Carbonic anhydrase inhibitors: stacking with phe131 determines active site binding region of inhibitors as exemplified by the X-ray crystal structure of a membrane-impermeant antitumor sulfonamide complexed with isozyme ii. *J. Med. Chem.* **2005**, *48*, 5721–5727.

(63) Biswas, S.; Carta, F.; Scozzafava, A.; McKenna, R.; Supuran, C. T. Structural effect of phenyl ring compared to thiadiazole based adamantyl-sulfonamides on carbonic anhydrase inhibition. *Bioorg. Med. Chem.* **2013**, *21*, 2314–2318.

(64) Avvaru, B. S.; Wagner, J. M.; Maresca, A.; Scozzafava, A.; Robbins, A. H.; Supuran, C. T.; McKenna, R. Carbonic anhydrase inhibitors. The X-ray crystal structure of human isoform II in adduct with an adamantyl analogue of acetazolamide resides in a less utilized binding pocket than most hydrophobic inhibitors. *Bioorg. Med. Chem. Lett.* **2010**, *20*, 4376–4381.

(65) Lolak, N.; Akocak, S.; Bua, S.; Sanku, R. K. K.; Supuran, C. T. Discovery of new ureido benzenesulfonamides incorporating 1,3,5-triazine moieties as carbonic anhydrase I, II, IX and XII inhibitors. *Bioorg. Med. Chem.* **2019**, *27*, 1588–1594.

(66) Akocak, S.; Lolak, N.; Nocentini, A.; Karakoc, G.; Tufan, A.; Supuran, C. T. Synthesis and biological evaluation of novel aromatic and heterocyclic bis-sulfonamide Schiff bases as carbonic anhydrase I, II, VII and IX inhibitors. *Bioorg. Med. Chem.* **2017**, *25*, 3093–3097.

(67) Lolak, N.; Akocak, S.; Bua, S.; Koca, M.; Supuran, C. T. Design and synthesis of novel 1,3-diaryltriazene-substituted sulfonamides as potent and selective carbonic anhydrase II inhibitors. *Bioorg. Chem.* **2018**, *77*, 542–547.

(68) Akocak, S.; Lolak, N.; Bua, S.; Turel, I.; Supuran, C. T. Synthesis and biological evaluation of novel N,N'-diaryl cyanoguanidines acting as potent and selective carbonic anhydrase II inhibitors. *Bioorg. Chem.* **2018**, *77*, 245–251.

(69) Lolak, N.; Akocak, S.; Bua, S.; Supuran, C. T. Design, synthesis and biological evaluation of novel ureido benzenesulfonamides incorporating 1,3,5-triazine moieties as potent carbonic anhydrase IX inhibitors. *Bioorg. Chem.* **2019**, *82*, 117–122.

(70) Genis, C.; Sippel, K. H.; Case, N.; Cao, W.; Avvaru, B. S.; Tartaglia, L. J.; Govindasamy, L.; Tu, C.; Agbandje-McKenna, M.; Silverman, D. N.; Rosser, C. J.; McKenna, R. Design of a carbonic

anhydrase IX active-site mimic to screen inhibitors for possible anticancer properties. *Biochemistry* **2009**, *48*, 1322–1331.

(71) Fisher, S. Z.; Aggarwal, M.; Kovalevsky, A. Y.; Silverman, D. N.; McKenna, R. Neutron diffraction of acetazolamide-bound human carbonic anhydrase ii reveals atomic details of drug binding. *J. Am. Chem. Soc.* **2012**, *134*, 14726–14729.

(72) Jitianu, A.; Ilies, M. A.; Scozzafava, A.; Supuran, C. T. Complexes with biologically active ligands. Part 8. Synthesis and carbonic anhydrase inhibitory activity of 5-benzoylamido- and 5-(3-nitrobenzoylamido)-1,3,4-thiadiazole-2-sulfonamide and their metal complexes. *Main Group Met. Chem.* **1997**, *20*, 151–156.

(73) *American Cyanamid*. Improvements in or relating to the manufacture of sulfonamides; Great Britain Patent GB769757, May 11, 1957.

(74) Almajan, L. G.; Supuran, C. T. Carbonic anhydrase inhibitors. Part 30. Complexes of 5-pivaloylamido-1,3,4-thiadiazole-2-sulfonamide with trivalent metal ions. *Rev. Roum. Chim.* **1997**, *42*, 593–597.

(75) Ilies, M. A.; Masereel, B.; Rolin, S.; Scozzafava, A.; Campeanu, G.; Cimpanu, V.; Supuran, C. T. Carbonic anhydrase inhibitors: aromatic and heterocyclic sulfonamides incorporating adamantyl moieties with strong anticonvulsant activity. *Bioorg. Med. Chem.* **2004**, *12*, 2717–2726.

(76) Khalifah, R. G. The carbon dioxide hydration activity of carbonic anhydrase. I. Stop-flow kinetic studies on the native human isoenzymes B and C. *J. Biol. Chem.* **1971**, *246*, 2561–2573.

(77) Draghici, B.; Vullo, D.; Akocak, S.; Walker, E. A.; Supuran, C. T.; Ilies, M. A. Ethylene bis-imidazoles are highly potent and selective activators for isozymes VA and VII of carbonic anhydrase, with a potential nootropic effect. *Chem. Commun.* **2014**, *50*, 5980–5983.

(78) Kabsch, W. XDS. *Acta Crystallogr., Sect. D: Biol. Crystallogr.* **2010**, *66*, 125–132.

(79) Adams, P. D.; Afonine, P. V.; Bunkóczi, G.; Chen, V. B.; Davis, I. W.; Echols, N.; Headd, J. J.; Hung, L.-W.; Kapral, G. J.; Grosse-Kunstleve, R. W.; McCoy, A. J.; Moriarty, N. W.; Oeffner, R.; Read, R. J.; Richardson, D. C.; Richardson, J. S.; Terwilliger, T. C.; Zwart, P. H. PHENIX: a comprehensive Python-based system for macromolecular structure solution. *Acta Crystallogr., Sect. D: Biol. Crystallogr.* **2010**, *66*, 213–221.

(80) Avvaru, B. S.; Kim, C. U.; Sippel, K. H.; Gruner, S. M.; Agbandje-McKenna, M.; Silverman, D. N.; McKenna, R. A short, strong hydrogen bond in the active site of human carbonic anhydrase II. *Biochemistry* **2010**, *49*, 249–251.

(81) Emsley, P.; Cowtan, K. *Coot*: model-building tools for molecular graphics. *Acta Crystallogr., Sect. D: Biol. Crystallogr.* **2004**, *60*, 2126–2132.

(82) Laskowski, R. A.; Swindells, M. B. LigPlot+: multiple ligand-protein interaction diagrams for drug discovery. *J. Chem. Inf. Model.* **2011**, *51*, 2778–2786.

(83) Krissinel, E.; Henrick, K. Inference of macromolecular assemblies from crystalline state. *J. Mol. Biol.* **2007**, *372*, 774–797.